Supplemental Data.

Supplemental Materials and Methods.

Bone Marrow Transplantation: For bone marrow transplantation experiments, female *LDLr*$^{-/-}$ recipient mice were obtained from the local animal breeding facility at the University of Leiden, Gorlaeus Laboratorium. Animals were exposed to a single dose of 9 Gy total body irradiation (0.19 Gy/min, 200kV, 4mA) using an Andrex Smart 225 Rontgen Source (YXLON International, Copenhagen, Denmark) one day before reconstitution with bone marrow cells from either wild-type C57Bl6/J mice obtained from Charles River Inc. or Hck/Fgr deficient mice on C57Bl6/J background, kindly provided by Dr. Clifford Lowell (University of California, Department of Laboratory Medicine in San Francisco CA, USA) and bred at the local animal facility of CNRS/IPBS, Toulouse; France. Drinking water with antibiotics (83 mg/l ciprofloxacin and 67 mg/l Polymixin) and 5 g/l sucrose was introduced one week before irradiation and supplied during the experiment. Mice were fed western type diet (WTD, 0.25% cholesterol and 15% cacao butter; Special Diet Services, Witham, Essex, UK) during 13 weeks, starting eight weeks after bone marrow transplantation and ending at sacrifice.

Perivascular Collar Placement, Adoptive Fluorescent Cell Transfer and Intravital Microscopy: Perivascular collars were placed in female *LDLr*$^{-/-}$ mice (n=5), as described elsewhere [1]. Mice were fed western type diet containing 0.25% cholesterol and 15% cacao butter (W. Special Diet Services, Witham, Essex, UK) four weeks before collar placement and throughout the experiment. Mice were anesthetized twelve weeks after collar placement, once advanced plaques had formed, and a mixture of DAPI labeled Hck/Fgr double knockout (dKO) and DiI labeled wild type (WT) BMDM (bone marrow derived macrophages) (10^6 cells each) was transferred by cardiac injection. Fifteen minutes after injection the left carotid was exposed for intravital microscopy recording during 1 minute, to quantify fluorescent labeled cell adhesion using an Olympus BX51 microscope equipped with a saline immersion 20X objective. Wounds were then sutured and animals allowed to recover from anesthesia and left one day until sacrifice to permit labeled cells diapedesis before analysis of post mortem cryosections by fluorescence microscopy.

Tissue Harvesting, Immunohistochemistry and Plaque Morphometry: Mice were anesthetized and sacrificed. Animals were perfused with PBS followed by 4% formaldehyde before dissection of heart, aorta, common carotid arteries, spleen, thymus and liver. Samples of spleen, thymus, liver, lung and bone marrow were collected for analysis of gene expression and histology. Three samples per organ were obtained, one of which was snapfrozen in liquid nitrogen and stored at −80°C. The other two samples were stored in 4% formaldehyde (4.5 times diluted Zinc Formal-Fix, Thermo Electron Corporation, Breda, The Netherlands) overnight before being embedded one in paraffin and the other in OCT compound (Tissue-Tek, Sakura Finetek). Ten or five µm thick cryosections were obtained respectively from the aortic root or the carotids. Aortic root sections were stained using the MOVAT's pentachrome procedure. Corresponding sections on separated slides (advanced lesions) were stained for α-naphthyl acetate esterase to detectplaque monocytes and macrophages (Sigma-Aldrich); or with rat anti-Ly6G (1:200 Clone 1A8, BD Biosciences Pharmigen), Rabbit anti rat-biotin (Dako), ABC Alkaline Phosphatase (Vector Laboratories) and Vectastain Red (Vector Laboratories) for granulocytes. Arginase-1 (AAM; Arg-1 rabbit polyclonal, kindly provided by P Van Dijk, UM; 1:1250), and iNOS (CAM; 1:20, Abcam) stainings were done on intermediate lesions after antigen retrieval at pH6 and vizualisation

with G-a-Rb Brightvision-AP (Immunologic)/Vector Red (Vector Laboratories); palque cell apoptosis was visualized by caspase-3 rabbit polyclonal Ab staining (1:100; Cell Signaling) and vizualization with G-a-Rb Brightvision-HRP/DAB. Picrosirius red was used for quantification of collagen (advanced lesions). Cryosections from adoptive cell transfer, were analyzed by fluorescence microscopy. Sections were analyzed by two different blind observators, using the Leica Qwin Image Analysis Software, or ImageJ. All counterstains were done with hematoxylin.

Intravital microscopy
Leukocyte adhesion to the carotid artery was analyzed in WT versus *Hck*$^{-/-}$*Fgr*$^{-/-}$chimeras via intravital microscopy, as described previously [2]. The right jugular vein was canulated with a catheter for antibody and dye injection. After exposure of the left carotid artery, antibodies (1 µg) to CD11b (650NC, ebioscience), Ly6g (BioLegend), and Ly6c (ebioscience) were sequentially administered by i.v. injection to label various leukocyte subsets. Recordings were made 3 min after injection of each antibody. Finally, rhodamine 6G (100 µl of a 0.1‰ solution) was injected to label all circulating leukocytes. Intravital microscopy was performed using an Olympus BX51 microscope equipped with a Hamamatsu 9100-02 EMCCD camera and a 10x saline-immersion objective. For image acquisition and analysis Olympus CellR software was used.

Latex bead labelling and histochemical/flow cytometric analysis: Ldlr$^{-/-}$ chimeras were generated by transplanting either WT or Hck$^{-/-}$//Fgr$^{-/-}$ bone marrow following lethal irradiation. To specifically label Ly6c^{hi} monocytes, mice were intravenously injected with Latex beads (Polysciences) 18h after receiving chlodronate liposomes as described before [3]. Twenty four hours after labeling, mice were sacrificed; aortas excised and subsequently used for flow cytometry analysis. Aortas were enzymatically digested with Liberase TM (Roche) and single cell suspensions were stained with a mix of antibodies against CD45 ,CD11b, Ly6G, Gr1, F4/80 and CD3. Additionally, blood was analysed by flow cytometry to allow for a normalization of data generated. Hearts were taken for cryo-sectioning and mounted with DAPI to analyze number of Lx bead positive cells per aortic root section.

Flow Cytometry:
Single cell suspensions of blood, bone marrow and peritoneal cells harvested at sacrifice were stained with fluorescent label conjugated antibodies after lysis of erythrocytes in ice cold NH_4Cl (8.4g/l) $NaHCO_3$ (1g/l) EDTA (37mg/l) during 3 minutes. Antibodies (eBioscience: B220, CD11b, CD3e, CD19, CD25, MHCII, CD8a, FoxP3; BD Pharmingen: Ly6G, CD11c, B220, CD11b, CD4; Miltenyi: Ly6c and Biolegend: F4/80) were used after Fc receptor blockage with CD16/32 blocking antibody (eBioscience). A FACSCanto II (BD Biosciences) flow cytometer coupled to FACSdivaTM software was used for acquisition and analysis of data. Whole blood samples were analyzed on a Sysmex blood cell analyzer (XT-2000i, Sysmex Europe GmbH, Norderstedt, Germany).

Cell Culture: Bone marrow macrophages derived from nonadherent precursors and peritoneal macrophages (PEM) were cultured in RPMI 1640 supplemented with L929 conditioned medium (LCM, 15%) or mouse recombinant M-CSF (20 ng/ml, ImmnunoTools, GmbH) as previously described [4]. The profibrotic capacity of macrophage conditioned medium was tested on a clonal population of mouse vascular smooth muscle cells (vSMC) derived from C57Bl6 aortic explants was kindly provided by Dr. Eric van der Veer (Leiden University Medical Center. Leiden, The Netherlands) and cultured for less than 5 passages on 1% gelatin and 10g/ml fibronectin coated wells with DMEM supplemented with 10% FCS, 2mM glutamine, 1% pyruvate, 100U/ml penicillin and 100g/ml streptomycin. For flow

chamber studies, we used human endothelial cells, (HAoEC, PromoCell) were grown in endothelial growth medium MV (PromoCell). Jurkat (JS-10) lymphocytes were cultured in DMEM supplemented with 10% FBS, 2mM glutamine, 1% pyruvate, 100U/ml penicillin and 100g/ml streptomycin.

Human monocyte/macrophage preparation: Human monocyte-derived macrophages were polarized as previously described **[5]**. Briefly, CD14-sorted human monocytes were cultured on glass coverslips in 6-well plates ($1.5x10^6$ cell/well) for 7 days in complete medium (RPMI 1640, 10% FCS, L-glutamine, penicillin-steptomycin) supplemented with 20 ng/ml hrM-CSF (Peprotech). Macrophages were polarized using either a mixture of LPS (15 ng/ml) and IFN-γ (100 U/mL-Roche) or IL4 (20 ng/mL-Miltenyi Biotec) for 18 h to obtain M1 and M2 polarized macrophages, respectively. Dendritic cells were differentiated from CD14-sorted human monocytes in 24-well plates ($5x10^5$ cells/well) in complete medium supplemented with hrGM-CSF (10ng/ml) and IL4 (20 ng/ml, Miltenyi Biotec). Murine B- lymphoma cells (A20, kindly provided by D. Hudrisier) was used as reference and were grown in complete medium supplemented with 50 µM beta-mercaptoethanol (Gibco).

Macrophage function assays

Efferocytosis: Apoptosis was induced in cell tracker CMTMR (5 µM, Molecular Probes) labeled Jurkat lymphocytes by incubation with staurosporine (1 µM, Sigma) for 2h. The degree of apoptosis was ≥ 70% as judged by AnnexinV and Propidium Iodide staining (BD biosciences) and flow cytometry. BMDM were incubated for 1h with LPS (10ng/ml) or complete medium, washed and incubated with labeled apoptotic cells (moi=20:1).

Phagocytosis: Phagocytosis was analyzed on a FACSCanto flow cytometer with FACSdiva™ software (BD Biosciences), extracellularly bound particles were distinguished from internalized particles by excluding cell aggregates from singlets in FSC vs FSC and SSC plots. In separated experiments, BMDM were incubated with FITC-coupled zymosan particles, (moi=20:1) opsonized by incubation with human IgG (13mg/ml in PBS, 20 min at 37°C). Cells were washed, fixed with paraformaldehyde (3.7%, Sigma) supplemented with 15 mM sucrose, rinsed with PBS and stained with TRITC-conjugated antibodies. Yellow (FITC- and TRITC-positive) extracellular zymosan particles were distinguished from green FITC-positive internalized particles. Cells were counted by fluorescence microscopy to determine the percentage of cells that had ingested at least one particle. For bead uptake, BMDM were grown in a 96 well plate at a density of approx 1.10^4 cells/well; cells were incubated for 24h at 37°C with fluorescently labeled beads at a ratio of 10:1 beads/cell. After incubation wells were washed 3x with buffer, and after fixing stained with Hoechst nuclear stain (1:5000); average bead uptake per cell was quantified by the BD Pathway 855 using BD Attovision v1.6 software.

*Lipid Loading***:** LDL was isolated from serum obtained from healthy volunteers using the density gradient ultracentrifugation method of Redgrave [6], oxidized with $CuSO_4$ (40 µM, 37°C, 24h) and dialyzed against PBS at 4°C as previously described [7]. After incubation with 50µg/ml of LDL or oxLDL in 12-well plates, BMDM ($1x10^6$ cells per well) were detached from the culture surfaces, suspended in PBS and frozen at −20°C for storage before further analysis. Cells were subsequently thawed and mechanically lysed by passage through a 22 gauge needle attached to a 10 ml syringe. Cell lysates were resuspended to 0.25 µg/l of protein. Cholesterol acetate (20 µg/ml in chloroform) was added as internal standard, to a total volume of 1200 µl and samples centrifuged at 3000 rpm for isolation of the chloroform fraction. Lipid extracts were subjected to HPTLC chromatography (Alltech/Applied Science) and analyzed for cholesterol content as described [8]. To assess total lipid uptake, OxLDL

was labelled with the fluorescent dye 1,1'-dioctadecyl-3,3,3',3'-tetramethylindocarbocyanine perchlorate (DiI) (Molecular Probes) by incubating 6 mg/ml DiI per ml of oxLDL, at 37°C overnight, in the dark, and subsequent removal of free DiI by size exclusion chromatography. BMDM (approx. 10^4 cells/well in 96 well plate) were incubated for 24h with 25 μg/ml DiI-labeled oxLDL and diI+ associated mean fluorescence index was measured after counterstaining of cells with Hoechst 33342 (Pierce) using the BD Pathway 855 microscope with Attovision vs1.6 software.
Immunomodulator release: BMDM were primed for 24h with IL-4 (20 ng/ml) or with Ifn-γ (100U/ml) and LPS (15 ng/ml). IL-10, IL-12p40, and TNF-α secretion into medium was measured by ELISA (Invitrogen) according to the manufacturer's protocol. As a measure of iNOS enzymatic activity, NO_2^- concentrations were determined in the cellular medium using Griess reagent and measured at 540 nm (Benchmark microplate reader; Bio-Rad).
Apoptosis: BMDM ($5x10^5$ cells/well) cultured on 0.2% gelatin coated 24-well plates, were serum-starved for 24h, incubated 48h in complete medium, harvested with EDTA (10 mM) and stained with Propidium Iodide (50 mg/ml) in PBS containing 2 mM $MgCl_2$, 50 units/ml DNAse free RNAse, 0.2% Triton X-100 (pH6.8). The same procedure was used for BMDM induced to undergo apoptosis by incubation with staurosporine (100 nM) and/or LPS (10 ng/ml) for 4h before harvesting.
Proliferation: The proliferation index was calculated as the ratio of cells in the S, G2 and M phases of the cell cycle, relative to the total number of cells. The experiments were done in triplicate and the results averaged. Data acquisition and analysis was done by flow cytometry using a FACSCanto II (BD Biosciences) coupled to FACSdiva™ software. No less than 10,000 cells were analyzed in each sample.

Macrophage morphology, migration, podosome rosette formation and matrix degradation:
Transwell experiments: 100 μl of Matrigel (BD Biosciences, batches from 8 to 10 mg/ml) or type I fibrillar collagen (2 mg/ml Nutacon, Leimuiden, The Netherlands) were poured in transwells (8 μm pores, BD Biosciences), polymerized for 30 minutes and 1h respectively at 37°C, and rehydrated with RPMI-1640 to obtain matrices. $5x10^4$ BMDM (n=3) were seeded in the upper chamber on top of the matrices for assessment of macrophage mesenchymal and amoeboid migration respectively, as previously described [9, 10]. Gelatin-FITC matrix degradation and podosome structures were assessed as described [6]. Rosettes of podosomes were considered large or small when their diameter was respectively bigger or smaller than 20m. When indicated a cocktail of protease inhibitors (PI, for composition see [9]) was added.
Wound healing assay: BMDM monolayers on 0.2% gelatin coated 24-well plates ($5x10^5$ cells per well) were serum-starved for 24h, scraped with a pipette tip, incubated 48h in complete medium and either photomicrographed for quantification of cell migration or collected for assessment of proliferation.
Cell morphology and polarization: PEM (peritoneal macrophages) were judged to be elongated or rounded when displaying an Elongation Index (EI, defined as the ratio of cell length to breadth) respectively greater or lower than 2 or 1.2, 36h after collection and culture. Cells showing more than three filopodial extensions, were judged to possess filopodia [11].

Quantitative qPCR
Classical and Alternative Macrophage Polarization: Immune polarization of BMDM ($5x10^5$ cells/well in 24-well plates) was induced by 24h incubation with either 100U/ml IFNγ/LPS (10 ng/ml) (Peprotech) or 20 ng/ml IL-4 (Peprotech).
Isolation of leukocyte subsets: Spleens were harvested from mice and single-cell suspensions were made by treating the spleens with liberase TL (Sigma) and filtering through a 70-uM

nylon filter (BD Bioscience). Splenic single-cell suspensions and blood were treated with red blood cell lysis buffer and non-specific FcR binding was blocked by incubating the cells with anti-CD16/32 (eBioscience). Subsequently cells were stained with anti-CD3, CD19, CD11c (eBioscience), NK1.1, CD11b, Ly6G (BD Bioscience) and Ly6C (Miltenji) fluorchrome coupled antibodies. Neutrophils ($CD11b^{+}$ $Ly6G^{+}$), monocytes ($CD11b^{+}$, $NK1.1^{-}$, $CD11c^{-/low}$, $Ly6G^{-}$, $Ly6C^{-/+}$),cDC ($CD11c^{high}$), T-cells ($CD3^{+}$) and B-cells ($CD19^{+}$) were sorted using a FACS ARIA I instrument (BD Bioscience). Populations were >95% pure.
qPCR: RNA was isolated using a Nucleospin RNA II kit (Macherey Nagel, Duren, Germany). cDNA was obtained with the iSCript RCDNA synthesis kit (BIO-RAD, Hercules, CA). Real-time PCR was done with a Taqman IQ RSYBR Green Super Mix (BIO-RAD, Hercules, CA) in a MyiQ Icycler (Biorad). Cyclophilin was used as house keeping gene. Primer sequences were as follows:

TNF:

- Forward: 5'-CAT CTT CTC AAA ATT CGA GTG ACA A-3'
- Reverse: 5'- TGG GAG TAG ACA AGG TAC AAC CC-3'

Hck:

- Forward: 5’- GCT CCA TAG ATC CGT CGT GCC ATT TCC -3’
- Reverse: 5’- GTT GTT TGG TCC CAG CTT GCT GGA GG -3’

Fgr:

- Forward: 5’- CAA GGC CGG ACT TCG TCC GTC TTT CC -3’
- Reverse: 5’- GAG AGC CTT ACT GGA ATC CCT CTT TAG C -3’

iNOS:

- Forward: 5’-CCT GGT ACG GGC ATT GCT-3’
- Reverse: 5’-GCT CAT GCG GCC TCC TTT-3’

IL-12p40:

- Forward: 5’-CGC AGC AAA GCA AGA TGT GT-3’
- Reverse: 5’-TGG AGA CAC CAG CAA AAC GA-3’

Arg-1:

- Forward: 5’-ATG GAA GAG ACC TTC AGC TAC-3’
- Reverse: 5’-GCT GTC TTC CCA AGA GTT GGG-3’

IL-10:

- Forward: 5’-TCT TAC TGA CTG GCA TGA GGA TCA-3’
- Reverse: 5’-GTC CGC AGC TCT AGG AGC AT -3’

MR:

- Forward: 5’-GCA AAT GGA GCC GTC TGT GC-3’
- Reverse: 5’-CTC GTG GAT CTC CGT GAC AC-3’

Cyclophilin:

- Forward: 5’-CAA ATG CTG GAC CAA ACA CAA-3’
- Reverse: 5’-TTC ACC TTC CCA AAG ACC ACAT-3’.

Samples were run in tri- quadriplicate and the comparative Ct method was used for analysis. Ct values were defined as the cycle number at which the fluorescence signals were detected.
*Quantitative real-time PCR Aorta***:** RNA was isolated from carefully dissected aortas by TRIzol (Invitrogen) in combination with the RNeasy mini kit (Qiagen). Expression was analyzed by multiplex, real-time one-step RT-PCR with the help of pre-developed multiplex TaqMan assays for m18s together with either mIL-6, mIL-10, MHC-II, and mCD206 (all from Applied Biosystems) according to the manufacturers’ protocols in a thermal cycler 7900HT (Applied Biosystems).

SDS-PAGE and western blotting analysis: Cells (10^6) were lysed with 100µl of boiling lysis buffer (62.5mM Tris HCl, pH 6.8, 2% SDS, 10% glycerol, 5% β-mercapto-ethanol, 0.002% Bromophenol blue) and protein lysates (10µl, except for A20: 40µl) were loaded onto 10 % SDS-PAGE, and transferred onto nitrocellulose membranes. The membranes were blocked with 5% BSA in TBS Tween 0.1%, and incubated with primary antibodies at 4°C overnight, anti-Hck (N-30, 1/1000), anti-Fgr (M-60, 1/1000) from Santa Cruz and anti-actin (20-33, 1/20,000 from Sigma-Aldrich). The membranes were washed three times with TBS Tween 0.1%, and exposed to the secondary antibodies at room temperature for 1h. Signals were detected by autoradiography using a chemiluminescence detection system and quantified using the Image J software.

Analysis of microarray data: For micro-array analysis, total RNA was extracted using the Guanidine Thiocyanate (GTC)/CsCl gradient method [12] and a NucleoSpin RNA II kit (Macherey Nagel, Duren, Germany). Comparison of gene expression was done for early (n=13) vs. advanced stable (n=16) lesions obtained after autopsy (Department of Pathology, University Hospital Maastricht, Maastricht, the Netherlands,) or advanced stable (n=21) vs. advanced unstable (n=23) lesions obtained upon surgery (Department of Surgery, Maasland Hospital Sittard, Sittard, the Netherlands). RNA concentration was determined using a Nanodrop ND −1000 and RNA quality assessed using the RIN (RNA integration number) values obtained with an RNA 6000 Nano/Pico LabChip (Agilent 2100) Bioanalyzer. Samples where the RIN number was lower than 5.6 were excluded from the study. The mean RIN was 7.20+/-0.49. Plaques were staged by histological analysis of adjacent slides according to Virmani [13] for which intimal thickening (IT) were characterized as early, thick fibrous cap atheroma (TkfcA) as advanced stable, and intraplaque hemorrhaged lesions (IPH) as advanced unstable lesions, respectively. Analysis of advanced stable vs unstable lesions was performed as detailed by Daissormont [14]. For analysis of early vs advanced stable lesions probe set normalization and summarization was performed using robust multi-array averaging RMA (RMA background subtraction, median polish summarization and quantiles normalization). Data normalization, summarization and statistical differences were assessed using respectively the R/Bioconductor packages affy [15] and Maanova [16]. Probes mapping to single gene IDs were selected using the highest Hyndmans type 7 IQR [17] after non specific removal of low entropy and low expression probes using MatLabs (Ver7.9) Bioinformatics Tool Box (Ver3.4). Genes with false discovery rate corrected $P \prec 0.05$ and fold change $\succ$ were considered differentially expressed and subjected to K-means with permutation cluster analysis using R/Maanova after cluster validation with SC2ATmd in MatLab [18]. Overrepresented biological categories within each cluster were identified using DAVID (Database for Annotation, Visualization and Integrated Discovery) [19]. Pathways were constructed with KEGG system retrieved information using the SOAP/WSDL based web serviced from withing MatLab's bioinformatics toolbox.

Supplemental Figure Legends:

Supplemental Figure 1.
A-B. Expression of Hck and Fgr in human atherosclerotic lesions. Hck/Fgr expression is upregulated in advanced versus early (A) and in vulnerable versus advanced stable (B) atherosclerotic lesions (****P≤0.001; ns: not significant).* **C**. Plasma IL-1α, IL-1β, IL-12p40, Eotaxin and MCP-1 levels are not affected in Hck/Fgr dKO chimeras (n=12). Correlation analysis of atherosclerotic lesion composition in Hck/Fgr dKO, $LDLr^{-/-}$ mice chimeras. **D+E**. Macrophage area correlated with plaque area in WT and dKO chimeras (Pval)WT≤0.0001, (Pval)dKO≤ 0.0001); there was no statistical difference between WT and dKO correlations (P = 0.5) (D). Necrotic core area correlated with plaque area in WT and dKO chimeras ((Pval)WT = 0.039, (Pval)dKO = 0.0061); there was no statistical difference between WT and dKO correlations (P = 0.4). (H*)* The 95% confidence band is shown by dotted lines. WT: black dots, dKO: white dots.
F+G. Expression of chemokine (receptor)s relevant to atherosclerosis. Bone marrow derived macrophages from dKO mice (filled circles) show equivalent mRNA expression of CCL2 and CCL5 as that from WT mice (open circles) (F), while similarly FACS sorted monocytes from dKO mice have unchanged chemokine receptor expression (G). Data are expressed as mean ± S.D. (n=3 biological replicates). WT: open circles; dKO: filled circles.

Supplemental Figure 2. Atherosclerotic Hck/Fgr dKO, $LDLr^{-/-}$ chimeric mice display blood $Ly6C^{high}$ monocytosis. Flow cytometry analysis of bone marrow cells showed essentially no differences in granulocyte and monocyte cell contents (A) and monocyte subsets (B) (n=5; sample duplicates per experimental unit). Surface expression of Ly6C is not influenced by the lack of Hck/Fgr in $Ly6C^{low}$ (C) and $Ly6C^{high}$ blood monocyte subsets (D) (n=5; duplicated samples per experimental unit). E. Representative histograms depicting Ly6C mean fluorescence intensity observed in WT (upper panel) and dKO blood monocyte subsets (lower panel). F-J. Normal absolute (F) and relative (G) blood granulocyte levels were observed in mutant chimeras. Similarly absolute (H) and relative monocyte blood monocyte numbers (I) did not differ between groups either. However dKO chimeras displayed a significant 1.5 fold increase in $Ly6C^{high}/Ly6C^{low}$ blood monocyte subset ratio compared to WT controls (J) (*P≤0.05). Of note: The percentage of $CD4^-$ and $CD8^-/CD4^+$ rDCs subsets in bone marrow was respectively 99.6 and 0.44% in WT versus 99.2 and 0.62% in dKO mice (data not shown here). WT: open circles; dKO: filled circles.

Supplementary Figure 3. DKO macrophages exhibited equivalent proliferation rates as WT macrophages (A) both at baseline and after LPS activation (mean ± S.D.; n=3). MRNA expression of classically activated macrophage markers iNOS and TNFα at baseline and in Ifn-γ/LPS or IL-4 primed BMDM was not affected by Hck/Fgr deficiency (B), while that of IL-12 tended to be elevated in dKO BMDM. Likewise, dKO BMDM showed similar mRNA expression of alternatively activated macrophage markers arginase-1 (Arg-1) and mannose receptor (MR) (C) (B+C: mean ± S.D.; n=4). At protein level, TNFα secretion by Ifn-γ/LPS primed dKO BMDM into medium was slightly elevated, whereas that of IL-12 was unchanged (E) and that of NO_2^- was reduced (F) (n=3; experiment done in twofold with essentially similar outcome; mean ± S.D.; *P≤0.05; **P≤0.01; ND: undetectable). WT: open circles; dKO: filled circles

Supplemental Figure 4. Effects of Hck/Fgr deficiency on macrophage functions relevant to atherosclerosis. The apoptotic susceptibility with staurosporine (STS, A) was not compromised in dKO compared to WT BMDM (mean ± S.D; n=3; experiment done twice with similar outcome). Macrophage uptake of fluorescent labelled beads expressed as average number of beads per cell (mean ± S.D; n=3; experiment done twice with similar outcome) (B), of IgG-opsonized zymosan particles (20 opsonized particles/cell; mean ± S.D.; n=3) (C) and of LDL or DiI labeled oxLDL (both 50 µg/ml, 24h), as judged by HPTLC analysis for cell-entrapped cholesterol (mean ±S.D.; n=3) (D) or DiI derived fluorescence (n=6) (E) were not affected as well. In contrast, the capacity to ingest apoptotic Jurkat cells (efferocytosis) was profoundly impaired with Hck/Fgr deficiency (mean ± S.D.; n=3) as assessed by high content microscopy analysis (F) or by flow cytometry (G) (*P≤0.05, **P≤0.01, ***P≤0.001). WT: open circles; dKO: filled circles

Supplemental Figure 5. Deficiency of Hck and Fgr renders macrophage differentiation more proteolytic. VSMCs were cultured for 48 hours with starvation medium (SM; open squares), normal medium (NM; filled squares), conditioned medium (CM) from dKO (open circles) or WT BMDM (closed circles), that had (red circles) or had not been stimulated with LPS (black circles). Despite similar proliferation rates (A), vSMCs on starvation medium (SM) and conditioned medium (CM) from dKO BMDM or WT LPS activated BMDM, displayed reduced extracellular deposition of collagen (B) and non-collagenous proteins (C), compared to vSMCs cultured in CM from WT BMDM. (n=4, *P≤0.05, **P≤0.01, ***P≤0.001).

Supplemental Figure 1

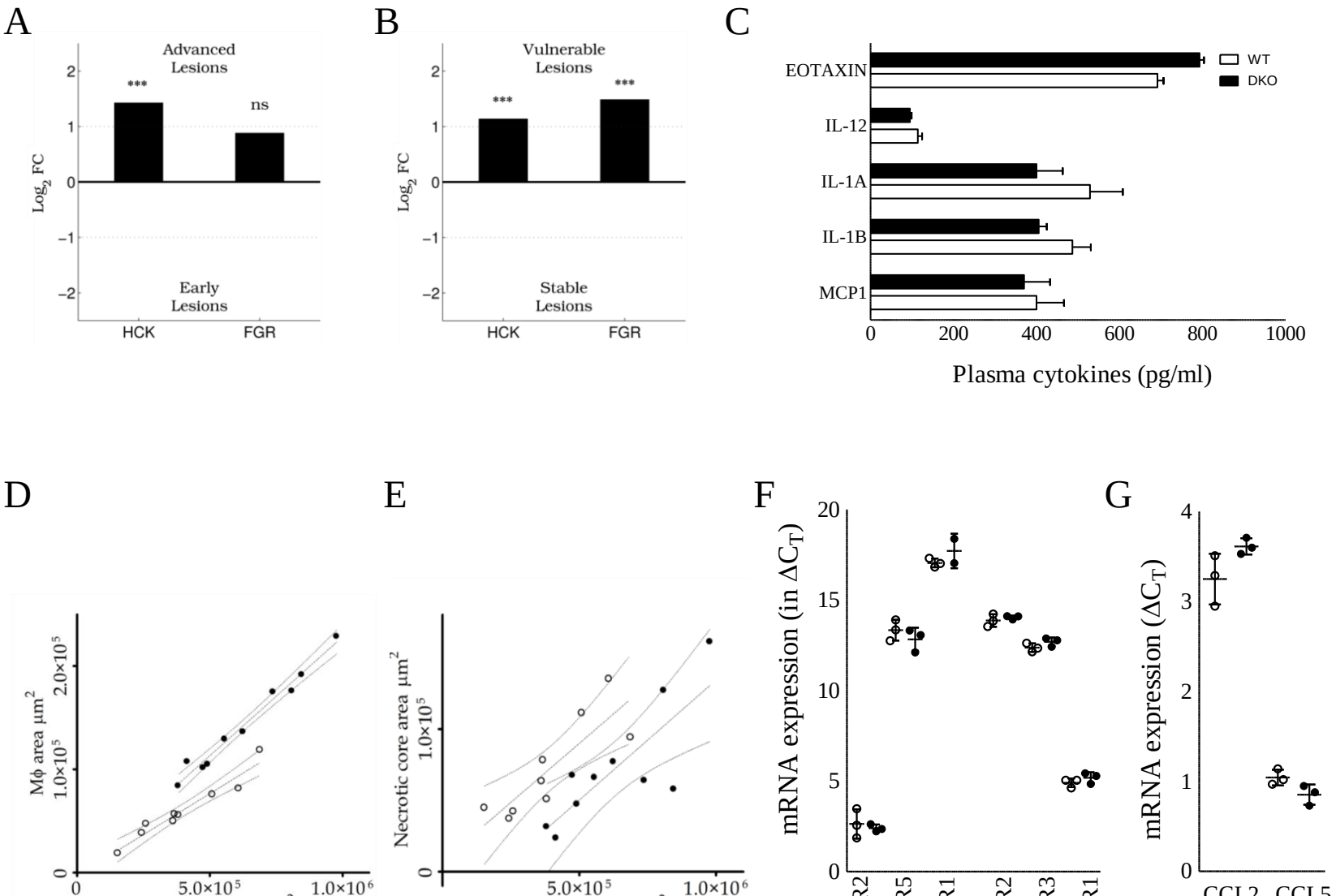

Supplemental Figure 2

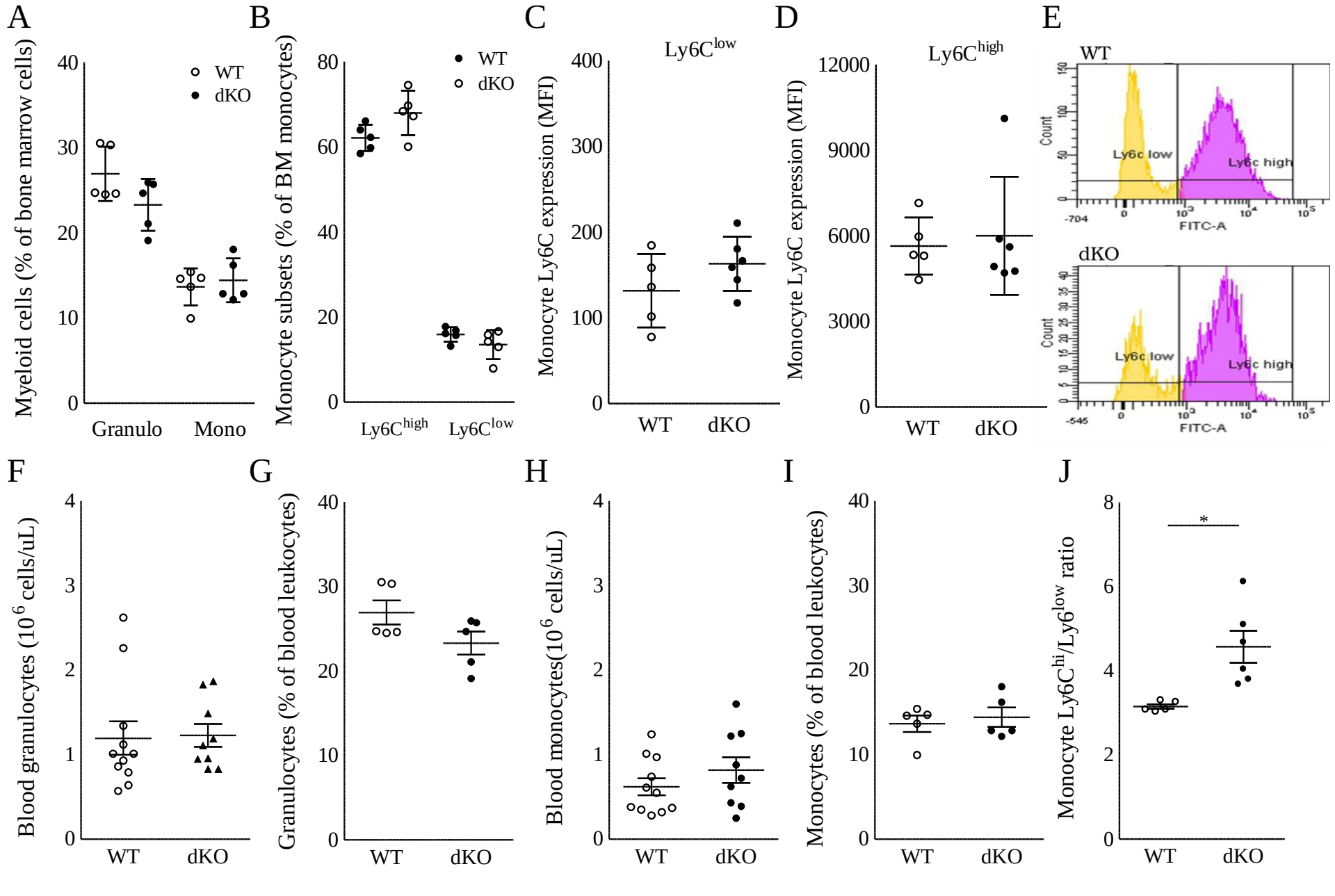

Supplemental Figure 3

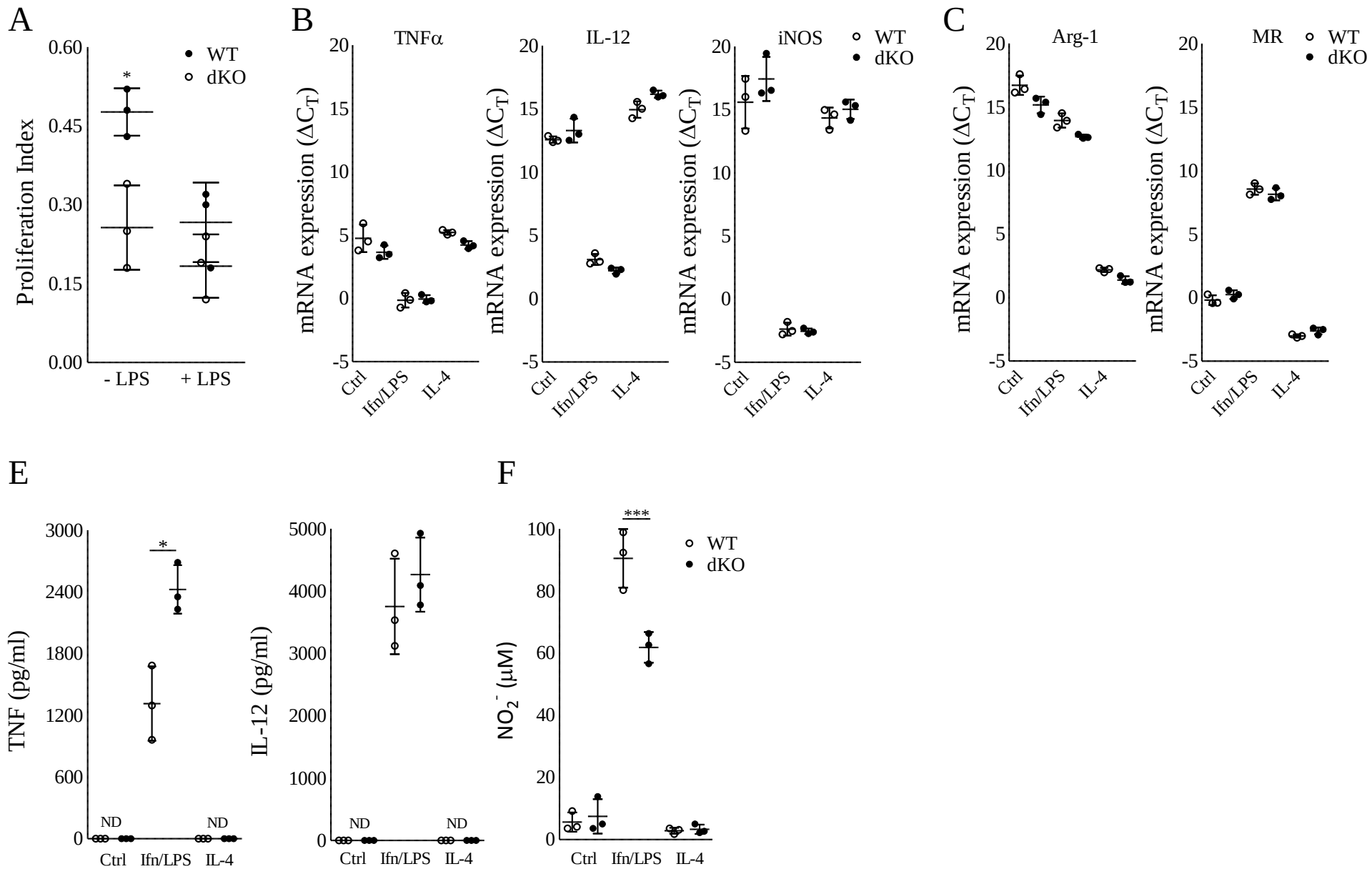

Supplemental Figure 4

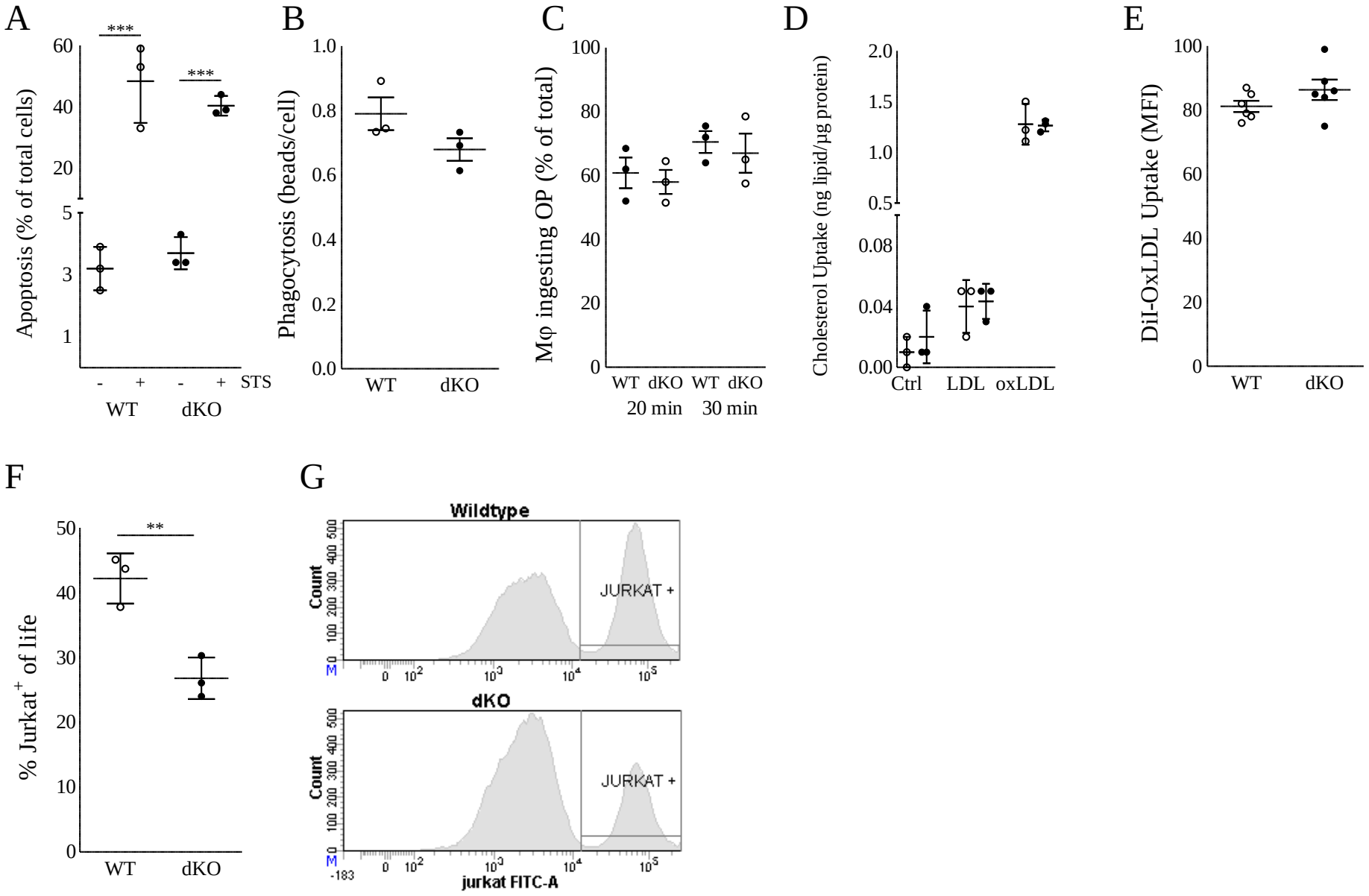

Supplemental Figure 5